

# AutoEncoder-Based Anomaly Detection for CMS Data Quality Monitoring

## Abstract

1 The monitoring of data quality in high-energy  
2 physics experiments is essential both during data  
3 acquisition and in offline analyses to ensure the re-  
4 liability of datasets. The Compact Muon Solenoid  
5 (CMS) experiment at the Large Hadron Collider  
6 (LHC) has recently implemented Data Quality  
7 Monitoring (DQM) at the granularity of individ-  
8 ual “luminosity sections” (LSs), each represent-  
9 ing about 23 seconds of data taking. This paper  
10 presents a novel application of AutoEncoders for  
11 anomaly detection in DQM, specifically targeting  
12 quantities associated with jets and missing trans-  
13 verse energy (MET). The developed method allows  
14 for the detection of anomalies at the LS level, which  
15 might be missed when examining integrated quan-  
16 tities. By automating the identification of anoma-  
17 lies, this approach enhances the efficiency and pre-  
18 cision of the DQM process, ultimately improving  
19 the quality of the datasets used for analysis.

## 20 1 Introduction

21 The Compact Muon Solenoid (CMS) [CMS Collaboration,  
22 2008] is a general-purpose detector at the Large Hadron Col-  
23 lider (LHC) at CERN. CMS is designed to study high-energy  
24 proton-proton collisions to better understand the fundamen-  
25 tal forces and particles that make up the Universe. The CMS  
26 apparatus is composed of a complex system of sub-detectors  
27 to detect the particles produced in a proton or ion collision.  
28 The only particles that CMS can not directly detect are neu-  
29 trinos, because of their very weak interaction with matter. To  
30 indirectly observe neutrinos, a kinematics observable called  
31 missing transverse energy (MET) is usually employed. MET  
32 is defined as:

$$\text{MET} = \left| - \sum_i \vec{p}_{T,i} \right|, \quad (1)$$

33 where  $\vec{p}_{T,i}$  is the transverse momentum of the  $i$ -th recon-  
34 structed particle of the final state.

35 Since the transverse momentum of the initial state is null,  
36 according to the law of conservation of momentum and en-  
37 ergy, MET is expected to vanish if all products of a collision  
38 were detected. However, because neutrinos and other weakly

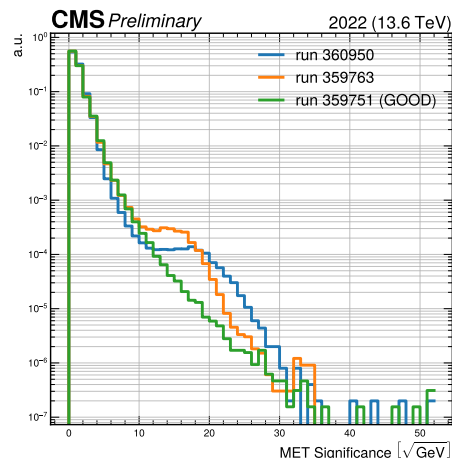


Figure 1: Histograms of a Monitor Element (MET Significance) for three different runs, one flagged *GOOD* and two presenting an anomaly, therefore flagged *BAD*.

interacting particles can escape the detector without being di- 39  
rectly detected, their presence result in a non vanishing miss- 40  
ing transverse energy value. 41

Particles that have a colour charge (like quarks and glu- 42  
ons) can not be directly observed as well. This is because 43  
a fundamental principle called colour confinement, accord- 44  
ing to which colour charged particles can not be isolated and 45  
they always combine in ways that ensure their overall colour 46  
charge is colour neutral. In order to obey colour confinement, 47  
quarks and gluons produced in strong interaction processes 48  
create other coloured particles to form hadrons clustered in 49  
*jets*, i.e. collimated groups of colourless objects [Ali and 50  
Kramer, 2011]. 51

LHC is a proton-proton collider. its operation consists 52  
of several phases, which can be broken down in three main 53  
stages: the filling of the machine with proton beams (which 54  
takes minutes); the subsequent collision phase, in which the 55  
beams are brought into collision, which can last several hours, 56  
typically until the proton population in the beams has fallen 57  
below a predefined threshold; the beam dump, in which 58  
the remaining beams are dumped and the machine is cycled 59

60 again. These three stages are collectively call in jargon a  
 61 *fill*. CMS takes data during the collision phase of a fill and  
 62 this data is gathered in “luminosity sections”, lumisections in  
 63 short (LSs), that are sub-sections corresponding to around 23  
 64 seconds of data taking during which the instantaneous *lumi-*  
 65 *nosity* (a quantity related to the collision rate) is almost constant  
 66 [CMS Collaboration, 2008]. LSs are grouped in *runs*,  
 67 of thousands of LSs.

68 Being CMS composed of various subsystems, each serv-  
 69 ing a specific purpose in particle detection and measurement,  
 70 issues in the different sub-detectors can arise due to various  
 71 factors, such as radiation damage, electronic noise, aging of  
 72 components and temporary malfunctions (such as tripping  
 73 of individual components). The monitoring of data quality  
 74 is therefore crucial both online, during the data taking, to  
 75 promptly spot issues and act on them, and offline, to provide  
 76 analysts with datasets that are cleaned against the occasional  
 77 failures that may have crept in. Data Certification (DC) is  
 78 the final step of quality checks performed by Data Quality  
 79 Monitoring (DQM) on recorded collision events. For each  
 80 run, experts monitor several reconstructed distributions called  
 81 Monitor Elements (MEs) to spot issues and anomalies in the  
 82 data. For quantities pertaining to hadronic jets and MET, an  
 83 issue in a few LSs could cause the entire run to be flagged as  
 84 problematic (*BAD*) and thus removed from the pool of good-  
 85 for-analysis data (*GOOD*).

86 Figure 1 shows the integrated (over the whole run) his-  
 87 togram illustrating a specific ME (MET Significance) for  
 88 three distinct runs—one categorised as *GOOD* and the other  
 89 two as *BAD*.

90 MET Significance is defined as:

$$91 \text{METSig} \equiv \frac{\text{MET}}{\sqrt{\text{SumET}}} = \frac{\text{MET}}{\sqrt{\sum_i |\vec{p}_{T,i}|}}. \quad (2)$$

92 This paper introduces a novel application of AutoEncoders  
 93 (AEs) for anomaly detection within the CMS DQM frame-  
 94 work. By exploiting unsupervised machine learning tech-  
 95 niques, we aim to automate the identification of anomalous  
 96 LSs. This approach enhances the efficiency and precision  
 97 of the DQM process, allowing for the isolation and removal  
 98 of problematic LSs, thereby improving the overall quality of  
 99 datasets available for analysis. Our method demonstrates sig-  
 100 nificant improvements in detecting subtle anomalies and en-  
 101 sures that data previously flagged as problematic can be re-  
 102 fined and utilised effectively, ultimately contributing to more  
 accurate and reliable physics analyses.

## 103 2 Methods

104 CMS has recently extended the possibility of accumulating  
 105 quantities monitored for data quality purposes per-LS to Jet  
 106 and Missing Energy (JME) MEs. This capability allows for  
 107 a higher granularity detection of anomalies, potentially en-  
 108 abling the saving of higher amounts of data from runs pre-  
 109 senting only a limited set of anomalous LSs. Given the high  
 110 number (order of thousands) of LSs to be analysed for each  
 111 run, an automated approach for DC is required.

112 Machine Learning (ML), particularly Neural Networks  
 113 (NN) [Goodfellow, 2016], can be implemented to this end.

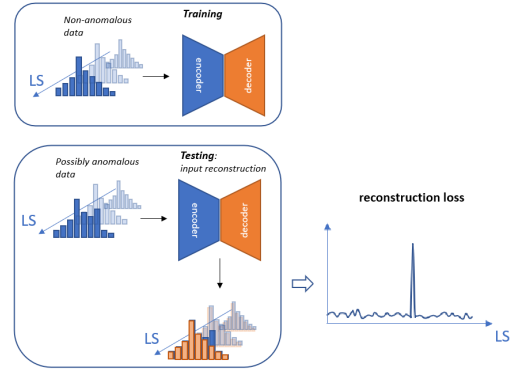


Figure 2: Scheme of training and testing steps for the models

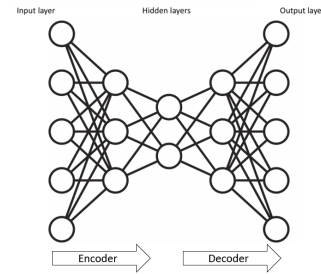


Figure 3: Structure of the dense Under-complete AE (the number of nodes is just indicative)

Therefore, to attack the problem, we employed unsuper- 114  
 115 vised ML models based on AutoEncoders (AE) [Hinton and  
 116 Salakhutdinov, 2006].

### 117 2.1 Input data and preprocessing

118 Given a specific ME, the input features to our models consist  
 119 of bins of the corresponding histogram, with each LS being  
 120 a single time sample. Thus, data is structured in the shape  
 121  $(\#bins, \#LS)$ .

122 Before feeding the models with training (and testing) data  
 123 we made a rescaling in the  $[0, 1]$  interval. This is a common  
 124 practice for this kind of models. Different rescalings are poss-  
 125 sible, but one that we found very effective is the following bin  
 126 by bin rescaling:

$$127 \hat{x}_{\text{train}} = \frac{x_{\text{train}} - \min(x_{\text{train}})}{\max(x_{\text{train}}) - \min(x_{\text{train}})}, \quad (3)$$

128 where the maximum and minimum are computed along the  
 129 time direction.

### 130 2.2 Models

131 Two types of AEs were developed: a dense Under-complete  
 132 AE and a Long Short-Term Memory (LSTM) Under-  
 133 complete AE.

134 The first model that was optimised is a dense Under-com-  
 135 plete AE [Hinton and Salakhutdinov, 2006] built us-  
 136 ing dense layers with three hidden layers in total, see Fig-  
 137 ure 3. The second model is the more complex LSTM Under-  
 complete AE [Wei *et al.*, 2023] schematised in Figure 4. This

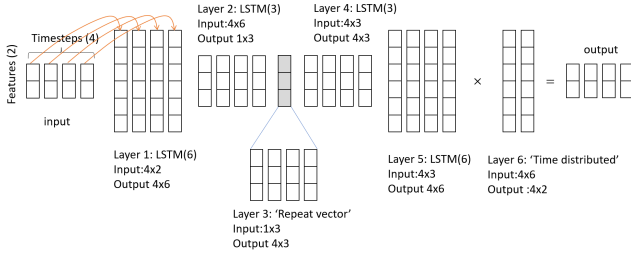


Figure 4: Structure of the LSTM Under-complete AE (the number of nodes is just indicative)

138 model is designed to handle sequential data, making it suit-  
 139 able for the time-series nature of DQM metrics. The struc-  
 140 ture is analogous to the dense Under-complete AE, with lay-  
 141 ers showing again a decrease followed by an increase of the  
 142 number of nodes but with the complication that each node is  
 143 an LSTM node, i.e. a Long Short-Term Memory recurrent  
 144 neural network (RNN). Due to the inherent recurrent nature  
 145 of LSTM, each node takes as input not a single time sample,  
 146 but a certain window of them. Thus, the output of each layer  
 147 is duplicated to enter each of the copies of every node of the  
 148 following layer. For the latent layer, a RepeatVector layer  
 149 is used to bring copies of the layer to the following decoding  
 150 layer.

### 151 2.3 Training and testing

152 Both the models were trained on non-anomalous data from  
 153 *GOOD* runs: histograms of specific MEs are fed to the model  
 154 with per-LS granularity to allow the AE to learn a normal,  
 155 non-anomalous behaviour of that specific ME, see Figure 2.  
 156 The training is performed via the minimisation of the recon-  
 157 struction loss, a measure of the distance between the input  
 158 and output of the AE. In this case, the reconstruction loss is  
 159 the mean squared error (MSE):

$$160 \text{MSE} = \frac{1}{n} \sum_{i=1}^n (y_i - \hat{y}_i)^2, \quad (4)$$

160 where  $y$  and  $\hat{y}$  are respectively the input and the output of the  
 161 AE, and  $n$  is the bin number.

162 Possibly anomalous runs under investigation are tested by  
 163 examining again the reconstruction loss: peaks in this func-  
 164 tion indicate LSs containing histograms that deviate from the  
 165 learned behaviour.

166 Optimised models (one for each ME) are paired with a  
 167 threshold value  $t_{hr}$  for the reconstruction loss that has been  
 168 tuned on a set of known anomalous runs. If the reconstruc-  
 169 tion loss exceeds this threshold during testing, it is considered  
 170 anomalous, and the corresponding LSs are removed.

## 171 3 Results

172 The models are tested in this example on a run (360950) that  
 173 was flagged *BAD* by JME due to the presence of an anomaly  
 174 visible in histograms of many different MEs, see e.g., Fig-  
 175 ure 1. By analysing the per-LS MET Significance for the run  
 176 via the dense Under-complete AE, a peak is observed in the

reconstruction loss corresponding to a specific LS (Figure 5). 177  
 The threshold for this model,  $t_{hr_{dense}} = 0.1$ , is passed. 178

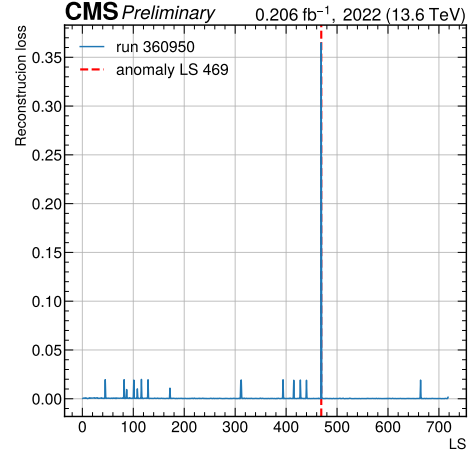


Figure 5: Reconstruction loss by the dense Under-complete model for an anomalous run showing a high peak corresponding to LS 469

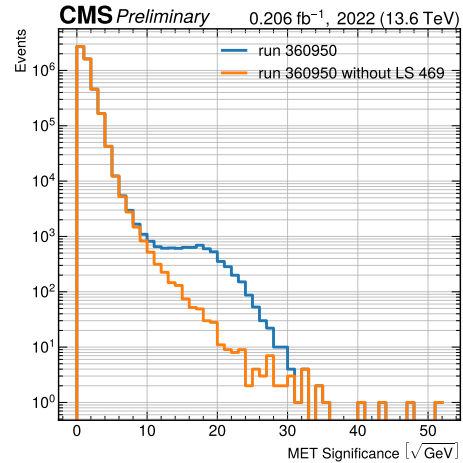


Figure 6: Histogram of an anomalous run before and after the removal of the identified anomalous LS

179 Once the anomalous LS is identified, it is removed from  
 180 the run. The resulting histograms for the *BAD* run show how  
 181 the cause of the MET Significance anomaly was isolated to a  
 182 specific LS, as shown in Figure 6. The exclusion of the iden-  
 183 tified anomalous LS results in the remaining data no longer  
 184 exhibiting the anomaly.

185 As a second example, we consider a run presenting an anal-  
 186 ogous anomaly, Figure 7. When tested with the dense Under-  
 187 complete model, only a major peak in the reconstruction loss  
 188 is visible, along with smaller peaks not relevant according  
 189 to the predefined threshold, Figure 8. When the only rele-  
 190 vant LS is removed, the resulting histogram still presents an

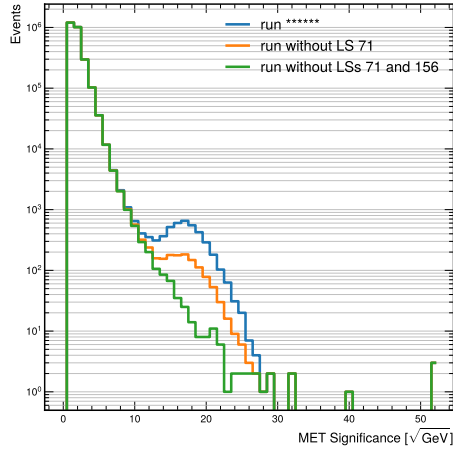


Figure 7: Histogram of an anomalous run before and after the removal of the identified anomalous LSs. The orange histogram represents the result after removing the LS identified by the dense Under-complete model, while the green one shows the result after removing both LSs identified by the LSTM Under-complete model

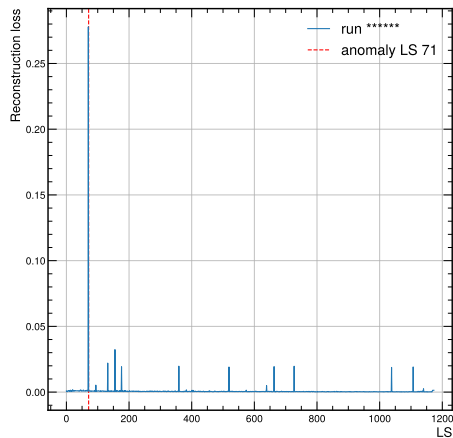


Figure 8: Reconstruction loss by the dense Under-complete model for an anomalous run showing a high peak corresponding to LS 71 above our fixed threshold for anomalies

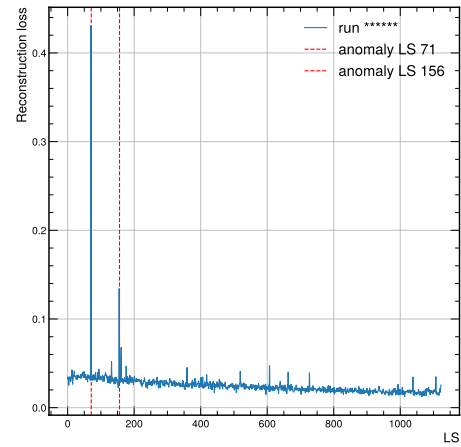


Figure 9: Reconstruction loss by the LSTM Under-complete model for an anomalous run showing a high peak (LS 71) and a second less pronounced peak (LS 156). Both are above our fixed threshold for anomalies

anomalous shape, Figure 7 . As changing the threshold allows for the removal of the whole anomaly, we decided to test the more complex LSTM Under-complete AE on the run. The resulting reconstruction loss shows a more pronounced peak for a second LS, acceptable according to the threshold for the model,  $\text{thr}_{\text{LSTM}} = 0.1$ , Figure 9 .

The removal of both the major peaks results in the complete cleaning of the anomaly, Figure 7 . When inspecting the two identified LSs, it is apparent that both anomalies were affecting the same set of bins in the histograms, with the second one being less pronounced: this results in a suppression of the magnitude of the rescaled bins after (3), making the anomaly far less visible to the dense Under-complete model.

## 4 Conclusions

An AutoEncoder-based anomaly detection tool has been successfully developed and tested for DQM in the CMS experiment. This tool, capable of detecting anomalies at the per-LS granularity, significantly improves the data certification process by isolating problematic LSs within runs flagged as *BAD*. While some anomalies could be detected by simple comparisons with average values, the models presented, and in particular the LSTM AE, prove versatile and robust across different types of anomalies, enhancing the overall data quality.

The removal of the identified anomalous LSs ensures that the remaining data is reliable, and the recovery of data that would otherwise be discarded. This approach not only streamlines the DQM process but also increases the efficiency and accuracy of data used for physics analyses, demonstrating the potential of machine learning techniques in high-energy physics.

This work uses results that are part of a CMS Detector Performance Note (DP-note) [CMS Collaboration, 2023].

## References

[Ali and Kramer, 2011] Ahmed Ali and Gustav Kramer. Jets and qcd: A historical review of the discovery of the quark

191  
192  
193  
194  
195  
196  
197  
198  
199  
200  
201  
202  
203  
204  
205  
206  
207  
208  
209  
210  
211  
212  
213  
214  
215  
216  
217  
218  
219  
220  
221  
222  
223  
224  
225

226 and gluon jets and its impact on qcd. *The European Phys-*  
227 *ical Journal H*, 36:245–326, 2011.

228 [CMS Collaboration, 2008] CMS Collaboration. S08004.  
229 *JINST*, 3, 2008.

230 [CMS Collaboration, 2023] CMS Collaboration. An  
231 autoencoder-based anomaly detection tool with a per-ls  
232 granularity. Technical Report 2023/010, CMS DP, 2023.

233 [Goodfellow, 2016] I. et al Goodfellow. *Deep Learning*.  
234 MIT Press, 2016.

235 [Hinton and Salakhutdinov, 2006] G. E. Hinton and R. R.  
236 Salakhutdinov. Reducing the dimensionality of data with  
237 neural networks. *Science*, 313(5786):504–507, 2006.

238 [Wei *et al.*, 2023] Yuanyuan Wei, Julian Jang-Jaccard, Wen  
239 Xu, Fariza Sabrina, Seyit Camtepe, and Mikael Boulic.  
240 LSTM-autoencoder-based anomaly detection for indoor  
241 air quality time-series data. *IEEE Sensors Journal*,  
242 23(4):3787–3800, 2023.